**CHONDRULES AND OPAQUE PHASES IN UNEQUILIBRATED R CHONDRITES: A COMPREHENSIVE ASSESSMENT OF THEIR FORMATION.** K. E. Miller[1] (kemiller@lpl.arizona.edu), D. S. Lauretta[1], H. C. Connolly Jr.[1,2], E. L. Berger[3], and K. Domanik[1], [1]Lunar and Planetary Laboratory, University of Arizona, Tucson, AZ 85721, USA, [2]Kingsborough Community College and The Graduate Center of CUNY, New York, New York, 10016, USA and AMNH, Central Park West, New York, NY 10024, USA. [3]GCS-Jacobs-NASA Johnson Space Center, Houston, TX 77058, USA.

**Introduction:** Equilibrated Rumuruti (R) chondrites record an oxygen fugacity between 0 and 3.5 log units below the fayalite-magnetite-quartz buffer [1], and a sulfur fugacity ($fS_2$) 2 log units above the iron-troilite buffer [2]. They are more than an order of magnitude more oxidized than the ordinary chondrites [1], and orders of magnitude more sulfidized than solar values [3]. Although the R chondrites have the highest $\Delta^{17}O$ value of any meteorites [4], analyses of unequilibrated R chondrites indicate chondrule formation in an oxygen isotope reservoir similar to that of the ordinary chondrite chondrules [5-8]. We present the relationship of the R chondrite parent body to pre-accretionary volatiles O and S based on our analyses of unequilibrated R chondrite material in two thin sections from the meteorite Mount Prestrud (PRE) 95404.

**Methods:** Thin sections PRE 95404,19 and PRE 95404,21 were studied. Samples were analyzed on the University of Arizona's Cameca SX100 electron microprobe. Bulk analyses of silicate chondrules are averages of broad-beam (25 µm) measurements, avoiding visible sulfide phases. Bulk abundances of sulfide assemblages were calculated based on pixel counts of each mineral phase in high-resolution X-ray maps and the average of point EMP analyses of each mineral. Cu-bearing phases were analyzed on a JEOL 7600F field emission scanning electron microscope (FE-SEM) at Johnson Space Center (JSC). Electron transparent FIB sections were prepared and analyzed using JSC's FEI Quanta 3D 600 dual beam FIB-SEM and JEOL 2500SE 200kV field emission scanning transmission electron microscope, respectively. Liquidus, solidus, and $fS_2$ calculations for sulfide assemblages were commissioned from the Spencer Group Inc. using the FTmisc database in FactSage. Pressure and dust/gas calculations were modeled on previously outlined procedures [9].

**Results:** *Silicate chondrules:* Silicate chondrules in thin section (TS) 19 average 300 µm in diameter, while those in TS 21 average 400 µm. Between the two thin sections, a variety of textures and compositions are represented. Of the 19 chondrules measured, 12 are FeO-rich (>10 wt.%). In TS 19, non-porphyritic chondrules are rare, and are comprised of one radial pyroxene chondrule and a cryptocrystalline fragment. In TS 21, non-porphyritic chondrules make up approximately 8% of the chondrule population, and include cryptocrystalline, barred olivine, and transitional chondrules. The thin section also contains one layered chondrule, with an interior sulfide rim surrounded by a silicate layer and an exterior sulfide rim.

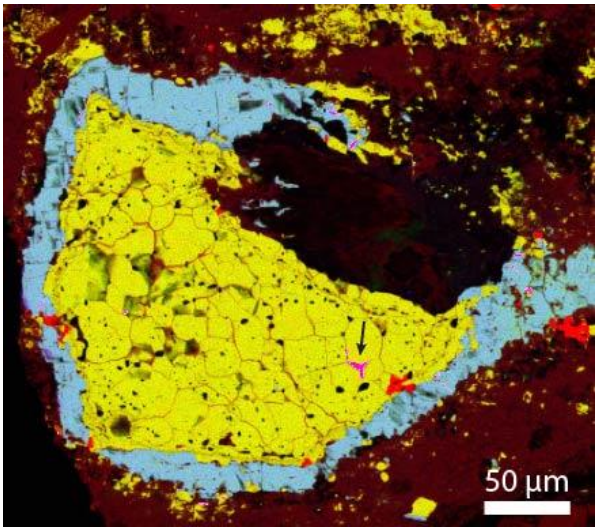


***Figure 1.*** *Composite X-ray map of sulfide assemblages in TS 19, with Fe (red), S (green), and Ni (blue). Pentlandite is blue-green, pyrrhotite is yellow, and iron oxide is bright red. A Cu X-ray map overlay is shown in pink. The black arrow indicates the Cu-rich region embedded in pyrrhotite that was analyzed via TEM.*

*Sulfide assemblages in matrix:* Both thin sections contain abundant, large (~200 µm) sulfide assemblages in the matrix. These assemblages generally have rounded shapes, and are primarily composed of pentlandite ($Fe_5Ni_{3.7}Co_{0.2}S_{8.1}$) and pyrrhotite ($Fe_{0.95}S$). Many assemblages are also associated with small (< 10 µm) iron oxide grains. In multiple instances, sulfide assemblages are found in petrologic relationships with silicate chondrules similar to that of compound chondrules, with one object deformed by the other.

Cu-rich lamellae are found in all pentlandite-bearing assemblages, and are found embedded in pyrrhotite in ~15% of assemblages. Detailed SEM analysis of an assemblage in TS 19 with Cu phases embedded in pyrrhotite (Fig. 1) indicates that the Cu-bearing mineral has both metal-rich and metal-poor regions. TEM analysis of a FIB section cutting across the lamella reveals a multi-component vein with varying Fe/S and Cu/S ratios and localized regions with Ni-enrichment.

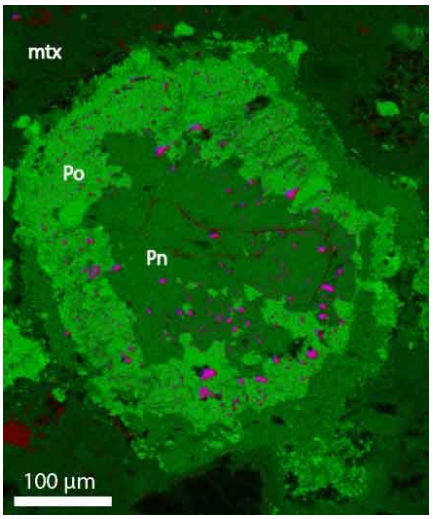


***Figure 2.*** *Composite X-ray map of a sulfide assemblage from TS 21, with Ca (red), Fe (green) and P (blue). Pentlandite (Pn), pyrrhotite (po) and matrix (mtx) are visible in shades of green, as marked. Ca-,P-rich inclusions are pink phases speckled throughout.*

Ca-, P-rich accessory phases are also common in sulfide assemblages, showing up as rounded features in the interior (Fig. 2). EMP analyses of these features in both thin sections are consistent with F-bearing merrillite, with an average formula of $Ca_{8.7}(Mg,Fe)_{1.4}Na_{0.9}(PO_{4.1})_7$ and an average F content of 0.3 wt.%. The presence of F may suggest a bobdownsite component [10, 11]. Some Ca-, P-bearing phases are Si-rich, with over 50 wt.% $SiO_2$.

In terms of their bulk composition, the Ni/Co ratio of assemblages is nearly constant, and close to the solar value of 21 [12]. Both elements are primarily carried by pentlandite. The Fe/Ni ratios are highly variable, consistent with the large variation in the pentlandite/pyrrhotite ratio of the assemblages. The S content is constant within each phase in most assemblages from their interior to their exterior.

*Sulfide assemblages in silicate chondrules:* Sulfide assemblages are occasionally found enveloped in or around the rim of silicate chondrules in TS 19. This occurrence is common in TS 21. Sulfide blebs associated with silicate chondrules often exhibit rounded shapes. They exhibit Cu-rich lamellae in 90% of chondrules with associated sulfide. Ca-, P-rich inclusions are also found.

**Discussion:** Although the texture, presence of mesostasis in some chondrules, and $Cr_2O_3$ content of olivine in both thin sections [13] is consistent with petrologic type of ~3.2 [8], a large proportion of chondrules are FeO-rich, suggesting that they are highly oxidized. These results are consistent with either preaccretionary oxidation, or low-temperature oxidation on the parent body. Mesostasis and silicate phases in chondrules suggest that the clast has not experienced aqueous alteration on a large scale. The oxidized state of many chondrules and large sulfide assemblages are therefore unlikely to be products of parent body aqueous alteration, and may be pre-accretionary.

Large sulfide nodules have been previously reported in CK4 and CK5 chondrites [14], where they are hypothesized to be the product of thermal parent body processes [15]. They are also found in the enstatite chondrites, where they are consistent with gas-solid corrosion reactions [16].

In the R chondrites, sulfide assemblages may have formed from gas-solid or aqueous corrosion of metal, or as melt droplets. If they were melt droplets, they may have been expelled from silicate chondrules during chondrule formation [17], or may have formed from separate, free-floating objects. The unequilibrated nature of the surrounding clast rules out melt formation on the parent body. We will present an assessment of each of the proposed formation methods in light of the observed characteristics outlined above.

The preponderance of evidence currently favors pre-accretionary melt formation. Merrillite in LL chondrites is hypothesized to form in magmatic processes, consistent with crystallization in the R chondrites following sulfide melt processes [18]. Thermodynamic calculations indicate that if the sulfide assemblages originated as melt droplets, they reached a peak temperature of at least 1138 °C, and are consistent with equilibrium $fS_2$ of $10^{-2.7}$ atm. These conditions remain true regardless of the original relationship between sulfides and silicate chondrules. These results are consistent with a total pressure of ~1 atm and dust enrichment three orders of magnitude above solar. Similar inclusions in sulfide blebs in silicate chondrules and free-standing sulfides argue in favor of a related origin for the two types of sulfide.

**References:** [1] Righter K. and Neff K. E. (2007). *Polar Science, 1,* 25-44. [2] McCanta M. C. et al. (2008). *GCA, 72,* 5757-5780. [3] Lehner S. W. et al. (2013). *GCA, 101,* 34-56. [4] Schulze H. et al. (1994). *Meteoritics, 29,* 275-286. [5] Greenwood J. P. et al. (2000). *GCA, 64,* 3897-3911. [6] Isa J. et al. (2011). *LPS XLII,* #2623. [7] Kita N. T. et al. (2015). *LPS XLVI,* #2053. [8] Miller K. E. et al. (2015). *LPS XLVI,* #2402. [9] Lauretta D. S. et al. (2001). *GCA, 65,* 1337-1353. [10] Tait K. T. et al. (2011). *The Can. Mineral., 49,* 1065-1078. [11] McCubbin F. M. et al. (2014). *Am. Mineral., 99,* 1347-1354. [12] Lodders K. (2003). *ApJ, 591,* 1220-1247. [13] Grossman J. N. and Brearley A. J. (2005). *MAPS, 40,* 87-122. [14] Rubin A. E. (1993). *Meteoritics, 28,* 130-135. [15] Tsuchiyama A. et al. (2002). *Geochem. J., 36,* 369-390. [16] Lin Y. and El Goresy A. (2002). *MAPS, 37,* 577-599. [17] Grossman J. N. and Wasson J. T. (1985). *GCA, 49,* 925-939. [18] Jones R. H. et al. (2014). *GCA, 132,* 120-140.